JBC RESEARCH ARTICLE

Characterizing unexpected interactions of a glutamine transporter inhibitor with members of the SLC1A transporter family

Received for publication, February 28, 2022, and in revised form, June 14, 2022 Published, Papers in Press, June 23, 2022,
https://doi.org/10.1016/j.jbc.2022.102178

Natasha J. Freidman[‡], **Chelsea Briot**[‡], **and Renae M. Ryan**[*]

From the Faculty of Medicine and Health, School of Medical Sciences, University of Sydney, Sydney, New South Wales, Australia

Edited by Karen Fleming

The solute carrier 1A family comprises a group of membrane proteins that act as dual-function amino acid transporters and chloride (Cl^-) channels and includes the alanine serine cysteine transporters (ASCTs) as well as the excitatory amino acid transporters. ASCT2 is regarded as a promising target for cancer therapy, as it can transport glutamine and other neutral amino acids into cells and is upregulated in a range of solid tumors. The compound L-γ-glutamyl-*p*-nitroanilide (GPNA) is widely used in studies probing the role of ASCT2 in cancer biology; however, the mechanism by which GPNA inhibits ASCT2 is not entirely clear. Here, we used electrophysiology and radiolabelled flux assays to demonstrate that GPNA activates the Cl^- conductance of ASCT2 to the same extent as a transported substrate, whilst not undergoing the full transport cycle. This is a previously unreported phenomenon for inhibitors of the solute carrier 1A family but corroborates a body of literature suggesting that the structural requirements for transport are distinct from those for Cl^- channel formation. We also show that in addition to its currently known targets, GPNA inhibits several of the excitatory amino acid transporters. Together, these findings raise questions about the true mechanisms of its anticancer effects.

The alanine serine cysteine transporters (ASCTs, designated as ASCT1/*SLC1A4* and ASCT2/*SLC1A5*) are widely expressed throughout the human body and represent a major neutral amino acid transport system (1–3). ASCT2 is also known to be overexpressed in tumors, along with other major transport systems including the large-neutral amino acid transporters (LATs; *SLC7/SLC43*) and other glutamine transporters belonging to the SLC38 family of sodium (Na^+)-coupled neutral amino acid transporters (SNATs) (4). ASCT2 supports tumor progression; pharmacological inhibition and/or genetic silencing of this transporter decreases cell cycle progression, induces apoptosis, and slows the growth of numerous malignancies (5–7). These effects of ASCT2 silencing/inhibition are generally attributed to the capacity of ASCT2 to transport the amino acid glutamine across the cell membrane, a critical metabolic and biosynthetic substrate in cancer cells (8–10). Many tumors display a distinct metabolic program characterized by dependence on glutamine for fast growth and accumulation of biomass (8–10).

The ASCTs are part of the solute carrier 1A (SLC1A) family, which also includes the human glutamate transporters known as excitatory amino acid transporters (EAAT1–5). The EAATs are critical in regulating synaptic concentrations of the major excitatory neurotransmitter glutamate and acidic amino acid transport throughout the periphery (11). Members of the SLC1A family assemble as trimers in the membrane and exhibit dual functionality by transporting amino acids while also allowing chloride (Cl^-) permeation (12–15). A range of anions are known to be able to permeate the SLC1A-associated Cl^- channel, including the physiologically relevant anion chloride (Cl^-) as well as a number of other anions that follow the permeability sequence, $SCN^- > NO_3^- > I^- > Br^- > Cl^-$ in order of most to least permeable (16–18). This anion conductance is thermodynamically uncoupled from substrate transport but requires substrate and Na^+ binding to be activated (14, 16, 19, 20). Despite their overall similarity, members of the SLC1A family have differing stoichiometries. The EAATs are concentrative acidic amino acid transporters in which substrate transport is coupled to the cotransport of three Na^+ ions, one H^+ ion and the countertransport of one K^+ ion (21). In contrast, the ASCTs function as Na^+-coupled obligatory exchangers of neutral amino acids (17, 22).

Given the role of ACST2 in cancer biology, inhibitors have been developed as tools in functional studies and potential therapeutics. Anti-ASCT2 monoclonal antibodies and siRNA-based inhibitors have been explored, as have several classes of small-molecule inhibitors. The first inhibitors were designed similarly to the EAAT inhibitor known as DL-threo-beta-benzyloxyaspartate (DL-TBOA). This compound comprises an aspartate backbone that binds the substrate-binding site and a hydrophobic substituent of the side chain to interfere with the closure of a domain known as hairpin loop 2 (HP2), which acts as the "gate" of SLC1A transporters (23). Analogously, ASCT2 inhibitors based on substrates such as serine and glutamine have been developed (19, 24, 25). Following the development of the glutamine analogs, a related diaminobutanoic acid scaffold was explored, from which a lead

[‡] These authors contributed equally to this work.
[*] For correspondence: Renae M. Ryan, renae.ryan@sydney.edu.au.

compound (termed V-9302) was identified in mammalian cell lines and tested in animal models (26). However, it was later shown that this compound is not an ASCT2 inhibitor but in fact blocks SNAT and LAT transporters (27). *In silico* screening of compounds in the substrate-binding site of ASCT2 has also led to the identification of alternative scaffolds. The most recent of these include two separate series of hydroxyprolines (28, 29), from which selected biphenyl esters reached unprecedented nanomolar potency. Notably however, these also bind ASCT1 and multiple EAATs with low micromolar affinity (29); ASCT2 inhibitors of sufficient selectivity and potency remain elusive.

The ASCT2 inhibitor which has been most widely used to probe the role of this transporter in a cancer biology context is the commercially available glutamine analogue, L-γ-glutamyl-*p*-nitroanilide (GPNA; Fig. 1) (24). A PubMed search for this compound yields over 100 results. GPNA binds to and inhibits glutamine transport *via* ASCT2 but is also known to inhibit SNAT and LAT transporters to a similar extent (24, 30, 31). Several aspects of the activity of GPNA require clarification to ensure correct interpretation of numerous cancer biology studies. First, because of difficulties in expression of human ASCT2 (hASCT2), prior electrophysiological characterization of GPNA has been performed on the rat homolog of ASCT2 (rASCT2) (32), and it is not known whether GPNA binds hASCT2 or rASCT2 as a competitive inhibitor or as a transported substrate. Although its effects on cell viability are often attributed to reduction of amino acid uptake by ASCT2 and other transporters, if the compound entered the cell, it could interact with intracellular targets. For example, GPNA hydrolysis by the enzyme γ-glutamyltransferase generates the cytotoxic metabolite *para*-nitroaniline (33). Second, the effects of this compound on the Cl^- conductance of either rASCT2 or hASCT2 have not been examined. Disruptions of Cl^- homeostasis across the plasma membrane can affect membrane potential and osmotic balance and may contribute to the effects of GPNA effects in cancer cells (34, 35). Third, while GPNA is selective for ASCT2 over ASCT1 (32), we hypothesized that it may interact with other SLC1A transporters, given the substrate-binding site is highly conserved within the family (12, 13).

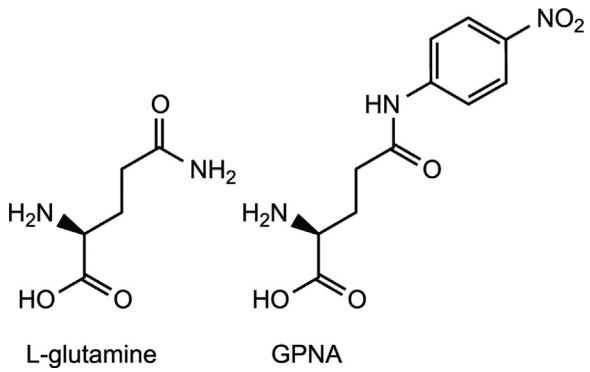

Figure 1. Chemical structures of L-glutamine and L-γ-glutamyl-*p*-nitroanilide (GPNA).

We expressed ASCT1, ASCT2, and EAATs in *Xenopus laevis* oocytes and directly compared their interactions with GPNA. We present evidence that GPNA acts as an inhibitor of EAAT1, EAAT2 and EAAT3, blocking both substrate transport and the leak of Cl^- conductance, which expands the known nonselective targets of this compound. We also present novel findings concerning the interaction of GPNA with ASCT2. To determine whether previous data generated using the rat isoform are applicable in the context of human disease, we compared the interactions of GPNA with hASCT2 and rASCT2 expressed in oocytes. Our results reveal that GPNA elicits distinct conductances in each of the two transporters. Strikingly, in oocytes expressing hASCT2, GPNA elicits currents comparable in magnitude and voltage dependence to those activated by substrates. Despite the activation of substrate-like currents, the results of radiolabeled efflux studies confirm that GPNA is a nontransportable inhibitor of ASCT2. This represents the first report of a nontransportable inhibitor interacting with an SLC1A transporter in this manner.

Results

GPNA binding has differential effects on hASCT2 and rASCT2

The neutral amino acid transporters ASCT1 and ASCT2 function as Na^+-dependent electroneutral exchangers. That is, for each neutral amino acid that enters the cell, there is a corresponding exit of another neutral amino acid in an Na^+-dependent manner (16, 17, 22, 36). In addition to this neutral amino acid exchange process, the binding of Na^+ and substrate to these proteins also activates an uncoupled Cl^- conductance, which allows the permeation of a range of anions including nitrate (NO_3^-), which is more permeant than Cl^- (16, 17). This conductance is comprised of a substrate-independent current ("leak" conductance) and a substrate-activated current (16, 17, 19). It is the activation and block of these conductances that generates measurable currents, which enables the use of electrophysiological recording as a readout of ASCT function.

Application of 1 mM of the substrate serine in an NO_3^- buffer to oocytes expressing rASCT2 and hASCT2 voltage clamped at −30 mV generates outward currents that represent the anion conductance activated during the transport process, while application of 1 mM of the nontransportable inhibitor benzylserine (19) results in an inward current that is consistent with block of the leak conductance of ASCT2 (Fig. 2, *A* and *B*). In contrast, application of 1 mM GPNA elicited outward current resembling substate-activated current in oocytes expressing both transporters (Fig. 2, *A* and *B*). While the currents at rASCT2 were of low amplitude, those at hASCT2 were comparable to the currents elicited by substrate alone. No measurable currents were recorded on water-injected oocytes under the same conditions, confirming the currents observed were ASCT2 mediated (Fig. 2*C*).

The currents elicited by GPNA over a range of membrane potentials (current–voltage relationships; IVs) were measured and compared with those elicited by substrate. Application of serine to both rASCT2 and hASCT2 in a buffer where nitrate

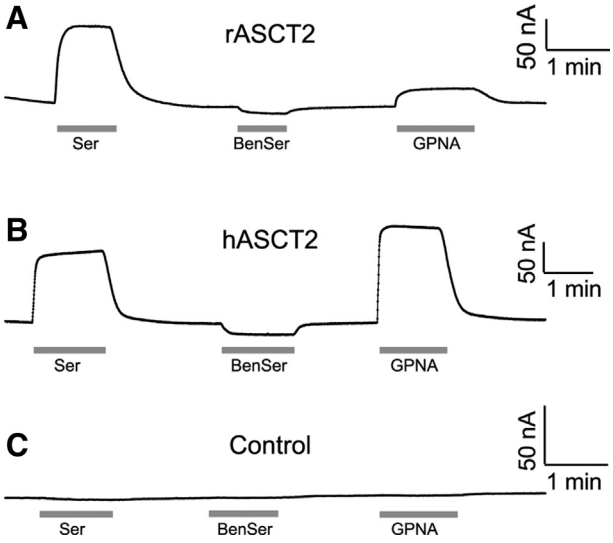

Figure 2. GPNA elicits distinct conductances in oocytes expressing hASCT2 and rASCT2. Representative traces of current elicited in oocytes clamped at −30 mV expressing rASCT2 (*A*), hASCT2 (*B*), and H_2O-injected control cells (*C*), in response to application of 1 mM serine, 1 mM GPNA, and 1 mM benzylserine in NO_3^- (representative of n ≥ 5 across ≥2 batches of oocytes). GPNA, L-γ-glutamyl-*p*-nitroanilide; hASCT2, human ASCT2; rASCT2, rat ASCT2.

(NO_3^-) is the predominant anion generates outward currents at most membrane potentials (Fig. 3, *A* and *B*). In oocytes expressing rASCT2, 1 mM GPNA activates small positive currents, although these were low in amplitude and thus ambiguous as to whether they reflected low-efficiency transport, leak block, or another effect (Fig. 3*A*). In contrast, application of 1 mM GPNA to oocytes expressing hASCT2 activates large outward currents at most membrane potentials that are comparable to the currents elicited by the predicted I_{max} of serine in buffers containing both NO_3^- and the physiologically relevant anion chloride (Cl^-) (90.0 ± 6.7% and 163.4 ± 35.3% of serine I_{max}, respectively) (Fig. 3, *B* and *D*). To investigate the binding mode of GPNA to hASCT2, we made use of a double mutation introduced into the substrate-binding site of rASCT2 (S466T/C467T), which knocks out glutamine transport *via* rASCT2 (32). The equivalent mutations were introduced into hASCT2 to generate a mutant herein referred to as "hASCT2 STCT." In this double-mutant transporter, GPNA cannot activate large outward currents, suggesting that GPNA does bind in the substrate-binding site (Fig. 3*C*). Indeed, GPNA can only activate 5.0 ± 1.1% of the current activated by the predicted I_{max} of serine, which is similar to rASCT2 (1.0 ± 0.7%; Fig. 3*D*).

The currents induced by GPNA were concentration dependent (Fig. 3, *E* and *F*), and GPNA exhibited an apparent affinity of 89.1 ± 17.9 μM for hASCT2 (Fig. 3*E*). As the GPNA currents in oocytes expressing rASCT2 are of low resolution, the apparent affinity of GPNA could not be measured by applying the compound independently. Instead, GPNA was competed with an EC_{50} concentration of glutamine, and an IC_{50} value of 38.7 ± 4.8 μM was established (Fig. 3*F*). Thus, GPNA appears to bind to both rASCT2 and hASCT2 with similar affinity, although with different activity. In addition, this activity was selective for ASCT2 over ASCT1; GPNA does

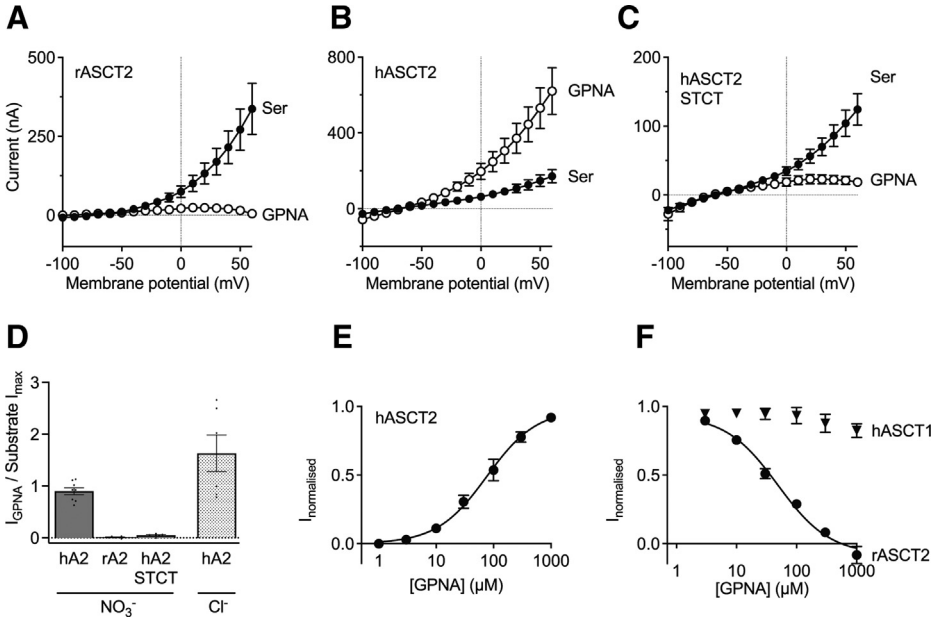

Figure 3. Characterization of ASCT2-mediated currents elicited by GPNA. *A–C*, current–voltage relationships elicited by L-serine (*closed circles*) and 1 mM GPNA (*open circles*) in oocytes expressing rASCT2 WT, hASCT2 WT, and hASCT2 S464C/T465T ("STCT") in NO_3^-. An EC_{30} concentration of serine was used for each transporter and corresponding controls (100 μM for hASCT2 and rASCT2 and 40 μM for hASCT2 STCT). *D*, current at +60 mV elicited by 1 mM GPNA in oocytes expressing ASCT2 transporters in NO_3^- or in ND96 (Cl^-), as indicated. Data were normalized to the predicted serine I_{max} in the relevant anion, for each cell. One outlier was removed by ROUT test (q = 1%). *E*, concentration–response curves of current elicited by GPNA in oocytes expressing hASCT2 at +60 mV in NO_3, normalized to the predicted GPNA I_{max} for each cell. *F*, inhibition–response curves of current activated by an EC_{50} concentration of substrate (90 μM serine for hASCT1 and 70 μM glutamine for rASCT2) at +60 mV in NO_3^-, competed with GPNA, in oocytes expressing hASCT1 (*inverted triangles*) and rASCT2 (*circles*). Data for each cell were normalized to substrate-activated current in the absence of GPNA. Data are mean ± SEM (n ≥ 3 across ≥2 batches of oocytes). ASCT2, alanine serine cysteine transporter 2; GPNA, L-γ-glutamyl-*p*-nitroanilide; hASCT2, human ASCT2; rASCT2, rat ASCT2.

not inhibit currents elicited by an EC_{50} concentration of serine in oocytes expressing hASCT1 (Fig. 3*F*).

To confirm the activity of GPNA on the various transporters, radiolabeled uptake and counter-transport experiments were performed, as these assays give a direct readout of substrate movement across the cell membrane. As described previously (30), application of 1 mM GPNA significantly inhibits both hASCT2-mediated and rASCT2-mediated uptake of an EC_{25} concentration of ^{3}H-L-serine to 34.3 ± 2.9% and 32.4 ± 3.5% of control, respectively, while no significant inhibition of ^{3}H-L-serine uptake was observed in oocytes expressing hASCT1 (Fig. 4*A*). To further probe the mechanisms by which GPNA interacts with ASCT2, we sought to determine whether external GPNA stimulates hASCT2- or rASCT2-mediated efflux of radiolabeled glutamine from oocytes. In obligatory exchangers, the ability to stimulate efflux is indicative of whether a compound is a transported substrate. In cells expressing both hASCT2 and rASCT2, external unlabeled glutamine was able to stimulate significant efflux of internal ^{3}H-L-glutamine, and this efflux was inhibited in the presence of GPNA (Fig. 4*B*). However, GPNA alone did not stimulate glutamine efflux above background in any condition. Together, these results suggest that GPNA binds both rASCT2 and hASCT2 but is not a transported substrate of either isoform, despite the activation of substrate-like currents in hASCT2.

GPNA acts as a leak blocker of EAATs

Given the similarity in the substrate-binding sites of SLC1A transporters, we hypothesized that GPNA may also bind to the EAATs, and this was confirmed to be the case (Fig. 5). Inward currents at positive membrane potentials indicate that a compound is a nontransportable blocker of SLC1A transporters, binding to the protein and blocking the leak conductance but not undergoing transport. IV relationships elicited by the application of GPNA to oocytes expressing EAAT1, EAAT2, and EAAT3 in NO_3^- were consistent with this (Fig. 5, *A*–*C*). While the voltage dependence was like that induced by the EAAT inhibitor DL-TBOA at all transporters,

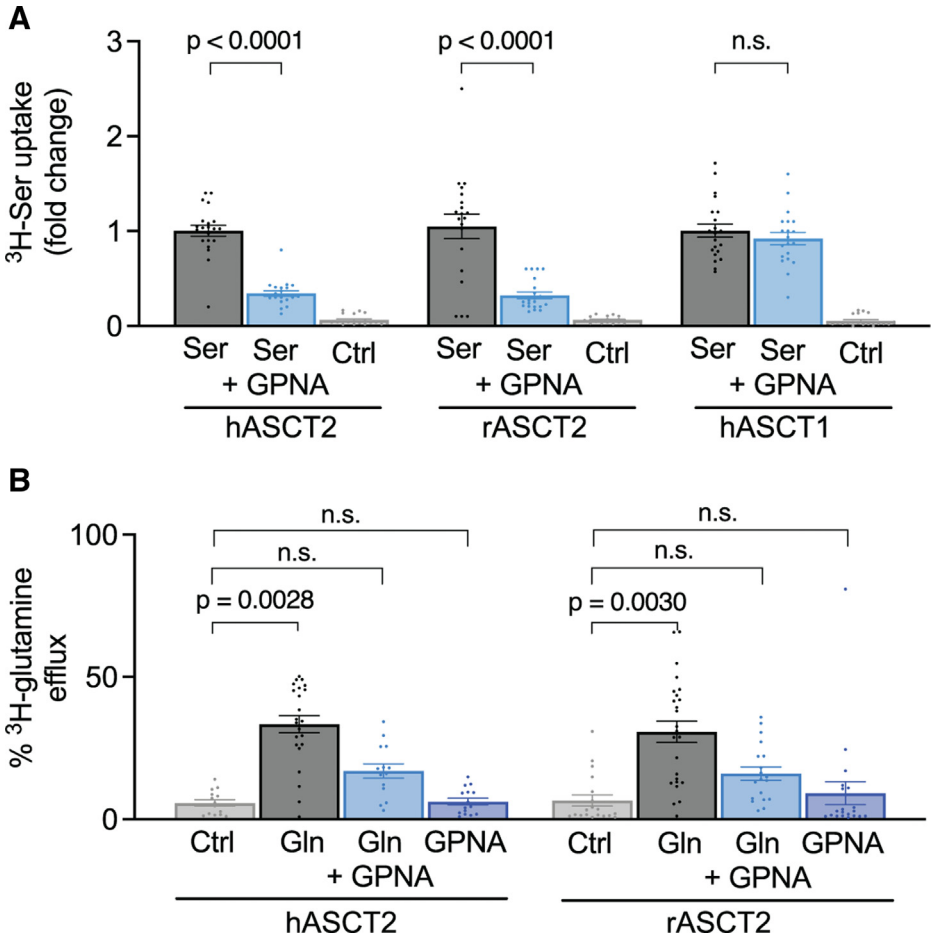

Figure 4. GPNA inhibits glutamine uptake by ASCT2 but is not a transported substrate. *A*, uptake of ^{3}H-L-serine ± 1 mM GPNA ("Ser + GPNA"; *light blue*) over 10 min by ASCTs and H_2O-injected negative control cells ("Ctrl"; *light gray*), normalized to the positive control (serine uptake by each transporter, for each batch of cells; "Ser"; *dark gray*). An EC_{25} concentration of serine was used for each transporter and corresponding controls (30 μM for hASCT1 and 80 μM for hASCT2 and rASCT2). *B*, efflux of injected ^{3}H-L-glutamine over 10 min by oocytes expressing ASCTs in external conditions of ND96 ("Ctrl"; *light gray*), ND96 + 300 μM unlabeled glutamine (*dark gray*), ND96 + 300 μM unlabeled glutamine + 1 mM GPNA (*light blue*), or ND96 + 1 mM GPNA (*dark blue*). Data across both parts are mean ± SEM (≥3 batches of oocytes, ≥4 oocytes per batch). *p* values were determined by two-way ANOVA and a Bonferroni post hoc test. ASCT2, alanine serine cysteine transporter; GPNA, L-γ-glutamyl-*p*-nitroanilide; hASCT2, human ASCT2; ND96, 96 mM NaCl, 2 mM KCl, 1 mM $MgCl_2$, 1.8 mM $CaCl_2$, 5 mM hemisodium–Hepes, pH 7.5; rASCT2, rat ASCT2.

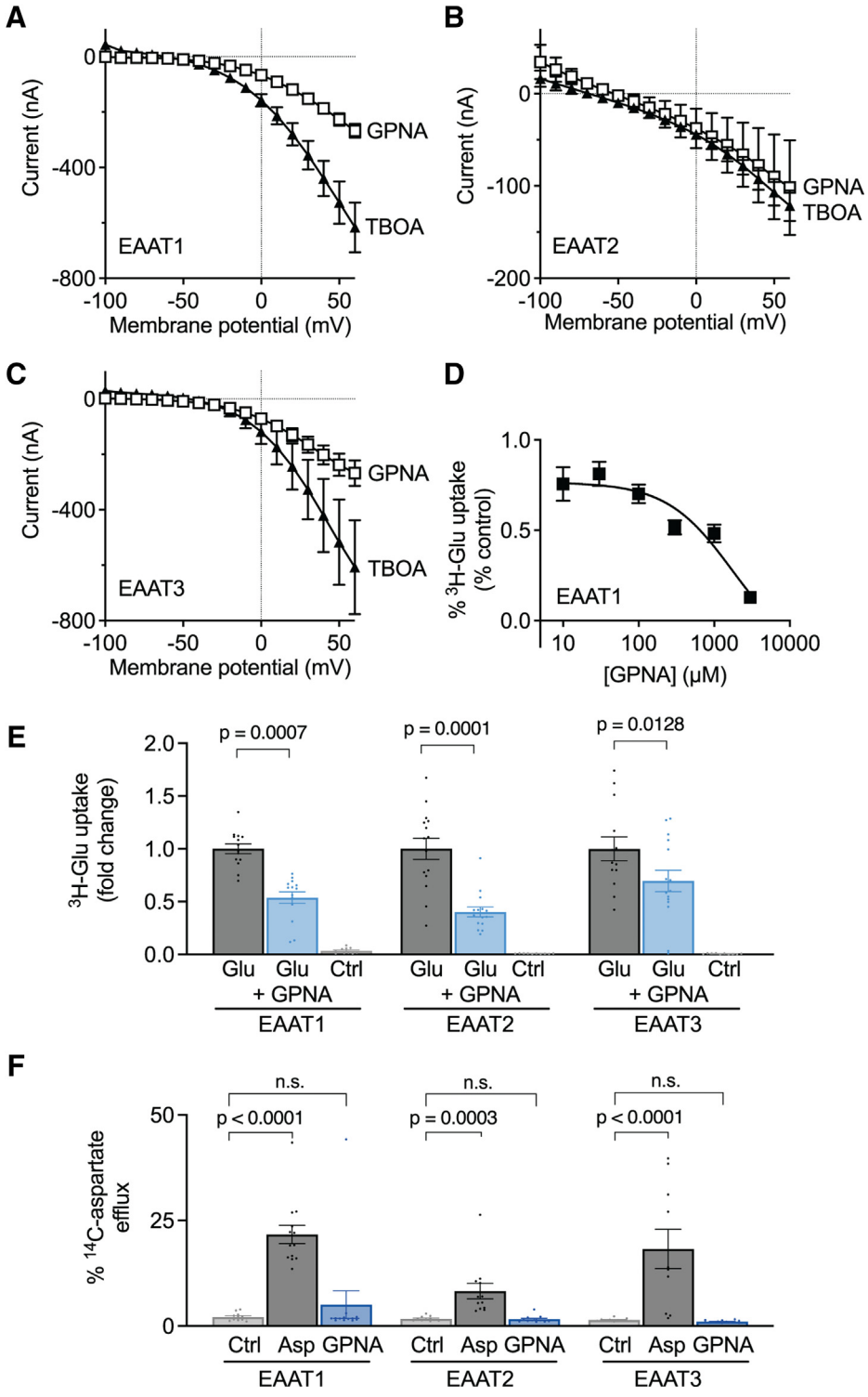

Figure 5. GPNA is a nontransportable inhibitor of EAATs. *A–C*, current–voltage relationships elicited by 30 μM DL-TBOA (*triangles*) and 1 mM GPNA (*open squares*) in oocytes expressing EAATs 1 to 3. *D*, inhibition–response curve of 10 μM 3H-L-glutamate uptake competed with GPNA in oocytes expressing EAAT1 over 10 min. *E*, uptake of 10 μM ^{3}H-L-glutamate ("Glu"; *dark gray*), ^{3}H-L-glutamate + 1 mM GPNA ("Glu + GPNA"; *light blue*) over 10 min by EAATs and H_2O-injected control cells ("Ctrl"; *light gray*). *D* and *E*, data were normalized to the positive control (glutamate alone). *F*, efflux of preloaded ^{14}C-L-aspartate over 45 min by oocytes expressing EAATs, in external conditions of ND96 ("Ctrl"; *light gray*), ND96 + 300 μM unlabeled L-aspartate ("Asp"; *dark gray*), or ND96 + 1 mM GPNA ("GPNA"; *dark blue*). Data are mean ± SEM (for *A–C*, total n ≥ 4 across ≥2 batches of oocytes, and for *D–F*, data from ≥2 batches of oocytes, ≥3 oocytes per batch). *p* values were determined by two-way ANOVA and a Bonferroni post hoc test. DL-TBOA, DL-threo-beta-benzyloxyaspartate; EAAT, excitatory amino acid transporter; GPNA, L-γ-glutamyl-*p*-nitroanilide.

the overall amplitude of the GPNA-induced leak block was lower. It was hypothesized that this may be because GPNA binds with lower affinity than DL-TBOA or simply blocks the leak conductance less efficiently than DL-TBOA. Indeed, concentration–response data collected from oocytes expressing EAAT1 indicate low-affinity binding of GPNA in the millimolar range (Fig. 5*D*).

Radiolabeled uptake data confirmed the results of electrophysiology on EAATs 1 to 3. Uptake of an EC_{25} concentration of glutamate in the presence of 1 mM GPNA was significantly reduced by >30% in oocytes expressing all three glutamate transporters (Fig. 5*E*). Radiolabeled efflux experiments were performed to confirm that GPNA does not independently stimulate substrate efflux from EAATs (Fig. 5*F*). While the EAATs primarily function as concentrative transporters, they can mediate substrate efflux under exchange conditions (where sufficient intracellular substrate and Na^+ are available). External aspartate induced significant efflux of internal ^{14}C-L-aspartate above background, whereas GPNA did not, confirming that GPNA does not undergo transport *via* the EAATs.

The conductances elicited by GPNA on SLC1A transporters are carried by anions

To identify the nature of the ion or ions generating the currents elicited by GPNA applied to oocytes expressing hASCT2 and EAAT1, IV relationships were measured in both standard NO_3^- and MES^- buffers (Fig. 6). The substitute anion Mes^- cannot permeate the Cl^- conducting pathway, thereby enabling the use of Mes^- to distinguish currents that are anion dependent from those that are not. For both 1 mM L-serine and 1 mM GPNA in oocytes expressing hASCT2, outward currents were observed in NO_3^- and abolished when the anion in the buffer was replaced with Mes^- (Fig. 6, *A* and *B*). This indicates that similarly to hASCT2 substrates, the outward current elicited by GPNA is due to activation of the intrinsic anion conductance of hASCT2. In oocytes expressing EAAT1, application of 1 mM aspartate in NO_3^- elicited outward currents reversing at −41.0 ± 1.3 mV (Fig. 6*C*). These represent the sum of transport current (a net influx of two positive charges per aspartate molecule transported) and substrate-activated anion conductance (NO_3^- flux through the Cl^- channel), both of which occur during the transport cycle. In contrast, 1 mM aspartate in Mes^- elicits negative currents that do not reverse direction at membrane potentials from −100 to +60 mV and represent EAAT1 transport current only (Fig. 6*C*). As previously mentioned, application of 1 mM GPNA in NO_3^- elicits inwardly rectifying currents suggestive of leak block in oocytes expressing EAAT1 (Fig. 6*D*). This effect is abolished when GPNA is instead applied in an Mes^- containing buffer (Fig. 6*D*). Data from oocytes expressing EAAT2 and EAAT3 showed the same trends as those observed in EAAT1 (Fig. 6, *E*–*H*). These data confirm that the currents elicited by GPNA on both the ASCTs and the EAATs are mediated by anion flux.

Discussion

Although the interactions of GPNA with hASCT2 and other SLC1A transporters have not previously been well characterized, this compound has been used extensively as an inhibitor of ASCT2 in human cancer studies. The effects of GPNA are generally attributed to inhibition of glutamine uptake by ASCT2, although it can also inhibit amino acid uptake by transporters from the SNAT and LAT families (30, 31). Our results reveal that alongside this inhibition of amino acid transport, GPNA activates currents in oocytes expressing hASCT2 comparable in magnitude to those elicited by substrate. This is the first description of a nontransportable compound eliciting currents at an SLC1A family member, which are comparable to those activated by amino acid substrates.

These findings may inform interpretation of the numerous cancer biology studies in which the compound GPNA is used. The activation of the anion conductance in hASCT2 is likely accompanied by water flux, as water is known to permeate the open channel of SLC1A transporters (15, 37–39). Ionic homeostasis, osmotic balance, and cell volume regulation play an important role in the control of the cell cycle, apoptosis, and migration and metastasis of cancer cells. Thus, excess anion and water flux across the membrane may compromise cancer cell viability (34, 35). While GPNA is not a viable drug candidate itself, novel cancer therapeutics that inhibit glutamine transport while also activating the chloride channel may be useful as anticancer agents. Modulation of the SLC1A Cl^- conductance may also have applications in other pathologies. For example, the Cl^- conductance of the EAATs regulates glutamate and anion homeostasis in the brain, and its dysregulation is associated with neurological phenotypes such as a motor disorder known as episodic ataxia (40–42).

Our finding that GPNA interacts with EAAT1, EAAT2, and EAAT3, blocking both substrate uptake and the leak anion conductance may also have relevance for its effects in cancer cells. Evidence suggests that like ASCT2, EAAT expression is associated with cancer progression, although it appears to be tumor promoting in certain contexts and tumor suppressive in others. In glioma and neuroblastoma, downregulation of EAAT1 and EAAT2 and associated reduction in glutamate uptake has been linked to tumor progression and invasion (43–45). In peripheral tumor types such as breast and gastric cancers, upregulation of EAAT1 and EAAT2 can support tumor metabolism and promote resistance to therapy and other stressors (46–50). In experimental cell models of such peripheral malignancies, modulation of EAAT activity by GPNA may contribute to the observed anticancer effects of this compound.

Because of the structural similarity between GPNA and the substrate glutamine (Fig. 1), it is thought that GPNA inhibits ASCT2 *via* a competitive mechanism. This hypothesis is supported by mutagenesis studies where a double mutation in the substrate-binding site has been shown to reduce GPNA-mediated inhibition of substrate-activated currents in oocytes expressing rASCT2 (32) and hASCT2 (this study). The differing conductances elicited at hASCT2, rASCT2, and the

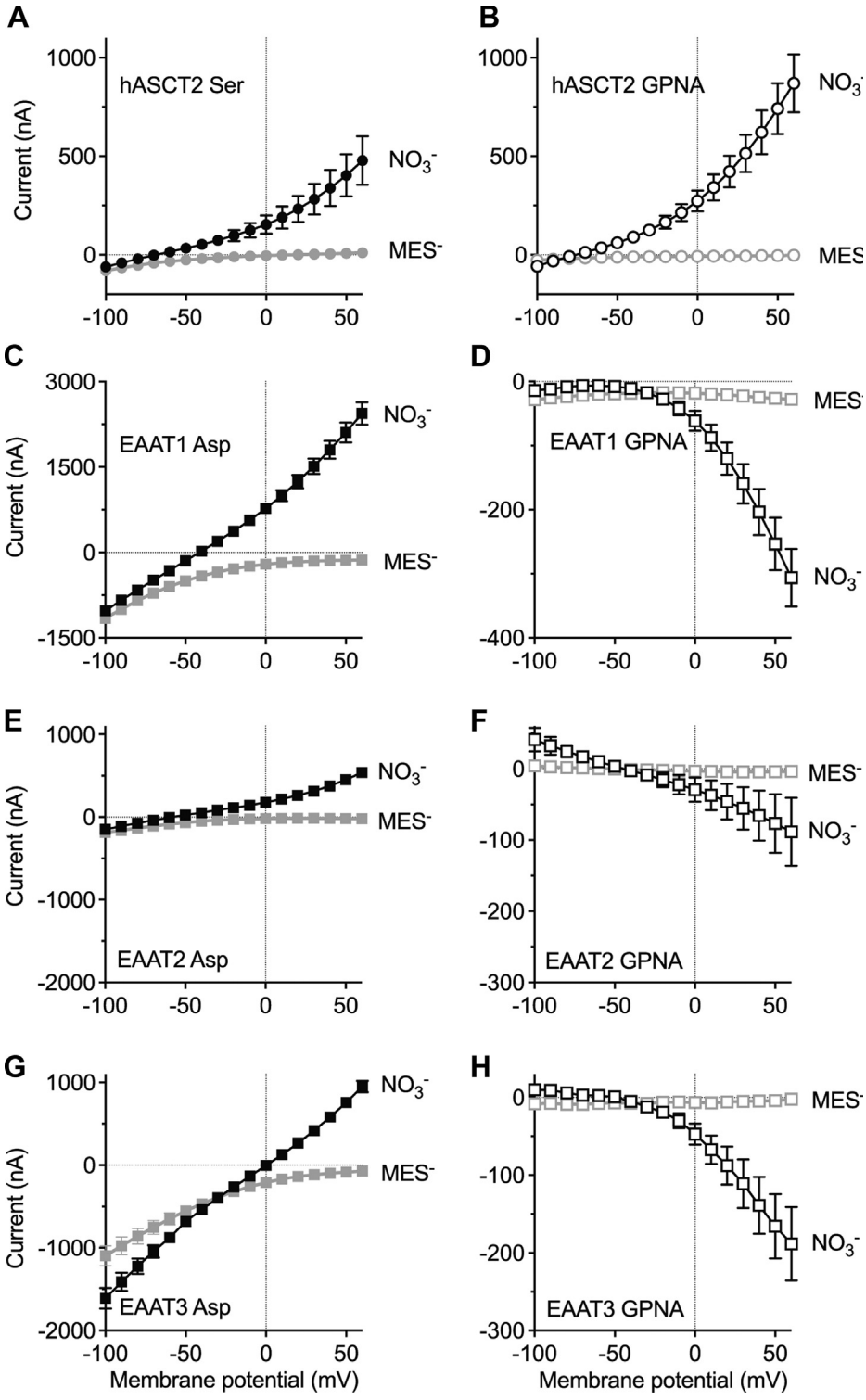

Figure 6. The conductance elicited by GPNA in oocytes expressing hASCT2 and EAATs 1 to 3 is carried by anions. *A* and *B*, current–voltage relationships elicited by 1 mM serine (*A*, "Ser"; *closed circles*) and 1 mM GPNA (*B*; *open circles*) in NO_3^-- (*black*) and Mes^- (*gray*)-containing buffers in oocytes expressing hASCT2. *C–H*, current–voltage relationships elicited by the application of 1 mM aspartate (*C*, *E*, and *G*, "Asp"; *closed squares*) and 1 mM GPNA (*D*, *F*, and *H*; *open squares*) in NO_3^-- (*black*) and Mes^-- (*gray*) containing buffers to oocytes expressing EAATs 1 to 3. Data are mean ± SEM (n ≥ 5 across ≥2 batches of oocytes). GPNA, L-γ-glutamyl-*p*-nitroanilide; hASCT2, human ASCT2.

EAATs observed in the present study may indicate differences in the positioning of GPNA in the substrate-binding site. During the characteristic "twisting elevator" movement of SLC1A transporters, a mobile transport domain moves downward relative to an anchored scaffold domain, causing the elicitation of a substrate-activated conductance as the transporter enters a Cl^--conducting state (ClCS) (15, 38, 51). For substrate transport to occur, the "gate" domain (HP2)

must first close over the binding site (23, 52). In contrast, competitive inhibitors like DL-TBOA prevent the closure of the HP2 gate, inhibiting the transport cycle and the Na^+-dependent leak conductance (23, 32). *In silico* modeling and structural studies of a homology model of ASCT2 exhibit two binding pockets for ASCT2 inhibitors (32, 53) (Fig. 7). "Pocket A" accommodates the hydrophobic bulk of inhibitors in a pose like that occupied by DL-TBOA in complex with the EAATs, wherein HP2 is in an outward-open state. In ASCT2, substitution of an arginine residue for cysteine in the binding site gives rise to an additional pocket (pocket B), which may result in differences in the ability of HP2 to close.

The leak block induced by GPNA binding to the EAATs suggests that GPNA induces these transporters to remain in an outward facing conformation, perhaps by occupying the substrate-binding site in a DL-TBOA-like pose (pocket A; Fig. 7), thereby preventing the downward movement of HP2 and other conformational changes required for transport. In contrast, GPNA-bound hASCT2 undergoes conformational changes sufficient to allow anion permeation with a similar voltage dependence to that induced by substrates but insufficient to allow the complete transport cycle. The structural foundations for the currents observed with rASCT2 are also ambiguous and may reflect an alternative intermediate state of the transporter domain. Previous functional studies within the SLC1A family have shown that the structural rearrangements required for anion channel formation are distinct from than those for complete substrate translocation (54–57), and a ClCS of the SLC1A prokaryotic homolog Glt_{Ph} has recently been resolved (15). In this ClCS, HP2 is closed, and a continuous aqueous pore appears at the interface of the transport and scaffold domains once the transport domain has undergone two-thirds of the substrate transport cycle. The stark variation in the conductances elicited by GPNA at hASCT2 and rASCT2 reveals functional differences between the two homologs, despite 79% sequence homology, and complete identity in regions proximal to the substrate-binding site (58). The ability of hASCT2 to enter into the ClCS whilst bound to GPNA, while rASCT2 cannot, suggests that residues in parts of the protein distal to the substrate-binding site, such as those in the interface between the two domains of the transporter, or in the channel itself, may underlie this species difference. It remains to be established whether the "transport-independent conductance" exhibited by hASCT2 is determined by differences in the extent of closure of HP2 and thus ease of relative movement between the two domains or ease of Cl^- movement through the channel conformation elicited by GPNA. Although structures of hASCT2 have been resolved by cryo-EM and predicted structures have been made available by AlphaFold (DeepMind) (59, 60), none are in complex with GPNA or in an open channel state.

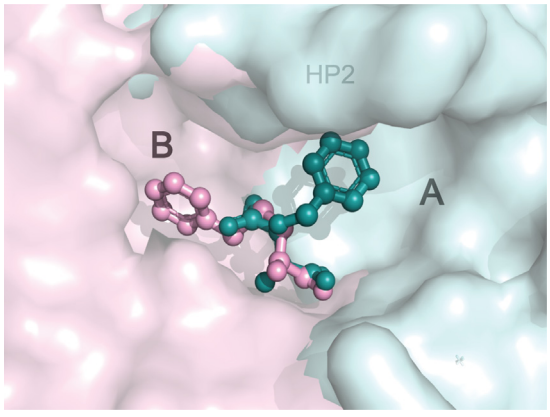

Figure 7. The ASCT2-binding site contains an additional hydrophobic pocket available for occupation by inhibitors. Superposed substrate-binding sites of Glt_{Ph} in complex with TBOA (*cyan sticks*; pocket *A*, PDB ID: 2NWW) and Glt_{Ph} R397C in complex with benzylcysteine (*pink sticks*; pocket *B*, PDB ID: 6BAV). Figure generated using PyMOL (62). ASCT2, alanine serine cysteine transporter 2; PDB, Protein Data Bank; TBOA, threo-beta-benzyloxyaspartate.

Together, the findings of this study represent the first observation of a nontransportable blocker of SLC1A transporters eliciting a substrate-like conductance. They also prompt caution in interpretation of the results of cell biology studies that use GPNA as an ASCT2 inhibitor. While the effects of this compound were previously thought to be mediated by transporters of glutamine and other neutral amino acids, this study highlights that they may in addition be mediated by interactions with the EAATs and by substantial disruption of chloride or water homeostasis within the cell, in addition to the known off-target effects.

Experimental procedures

All chemicals were purchased from Sigma–Aldrich (now Merck) unless otherwise stated.

Molecular biology

DNA encoding each transporter was subcloned into plasmid oocyte transcription vector. All DNA products were transformed into NEB 5-alpha competent *Escherichia coli* cells (New England BioLabs, Inc) according to the manufacturers' instructions and purified using the GeneJET Plasmid Miniprep Kit (Thermo Fisher Scientific). Site-directed mutagenesis was performed using the Q5 Site-Directed Mutagenesis Kit (New England BioLabs, Inc) according to the manufacturers' instructions. Primers were designed using the online tool NEBaseChanger (New England BioLabs, Inc) and synthesized by Sigma–Aldrich. The sequences of all complementary DNA products were confirmed by the Australian Genome Research Facility. Sequence-confirmed WT and mutant complementary DNAs were linearized using the restriction enzyme Spe1 (New England BioLabs, Inc). mRNA was transcribed by T7 polymerase using the mMESSAGE mMACHINE kit (Invitrogen).

Electrophysiology

Stage V oocytes were harvested from *X. laevis* and stored as previously described prior to injection (61), with the following modification to the methods: oocytes were defolliculated in 1.5 to 1.7 mg/ml collagenase A (Roche) at 18 °C for 30 to 60 min as required. All *X. laevis* surgical procedures have been approved by the University of Sydney Animal Ethics under the Australian Code of Practice for the Care and Use of Animals

for Scientific Purposes (protocol 2016/970). Individual stage V oocytes were microinjected with 2 to 10 ng of mRNA, as required (Nanoliter 2000; World Precision Instruments, Inc). Injection needles were made with 3.5′ Drummond glass capillaries (Drummond Scientific Co) using a microelectrode puller (Narishige). Injected oocytes were stored at 18 °C in ND96 (96 mM NaCl, 2 mM KCl, 1 mM $MgCl_2$, 1.8 mM $CaCl_2$, 5 mM hemisodium–Hepes, pH 7.5) supplemented with 50 μg/ml gentamycin, 2.5 mM sodium pyruvate, 50 μg/ml tetracycline, and 0.5 mM theophylline for a minimum of 3 days prior to testing *via* electrophysiological recording.

Current recordings were made using two-electrode voltage-clamp electrophysiology with a GeneClamp 500 amplifier (Axon Instruments) and a MacLab 2e chart recorder (ADInstruments) using LabChart software (version 8; ADInstruments) and a Digidata 1322A (Axon Instruments) controlled by an IBM-compatible computer with pClamp software (version 10.6; Molecular Devices). Solutions containing compounds of interest were applied to the oocytes through perfusion into a recording bath where the oocytes were held and washed out with recording buffer between applications. The amplitude of current activated by an applied compound-containing solution was measured as the difference between conductances recorded immediately before the application and during the application.

Recording buffers were varied throughout as indicated and were either ND96, ND96 with complete NO_3^- substitution for Cl^- (herein referred to simply as "NO_3^-"), or ND96 with complete anion replacement through sodium methanesulfonate substitution for NaCl and gluconate$^-$ substitution for all other Cl^- salts (referred to as "MES^-"). The recording bath was grounded using a salt bridge containing 3 M KCl and 30% agarose gel connected to a 3 M KCl reservoir. Oocytes were clamped at −30 mV. Voltage pulses at 10 mV intervals between −100 mV and +60 mV were applied to the oocytes every 150 ms in order to generate IV plots.

Concentration–response curves were plotted in GraphPad Prism 9 (GraphPad Software, Inc), and least-squares regression was used to fit current (I) to a derivation of the Michaelis–Menten equation,

$$\frac{I}{I_{max}} = \frac{[\text{Compound}]}{([\text{Compound}] + \text{EC}_{50})},$$

where I_{max} is the predicted maximal current elicited by the given compound and EC_{50} is the Michaelis constant (concentration required to elicit a half-maximal response). For inhibition–response curves, least-squares regression was used to fit current to the below derivation of the Michaelis–Menten equation for inhibition of transport,

$$\text{I} = \text{Bottom} + \frac{\text{Top–bottom}}{1 + \frac{X}{IC_{50}}},$$

where "bottom" and "top" refer to the lower and upper plateaus in the curve, respectively, IC_{50} is the inhibitor concentration required to elicit half-maximal inhibition and X is the applied inhibitor concentration. For all electrophysiological data, SEM calculated from all datapoints is displayed.

Radiolabeled uptake

Oocytes were injected with RNA-encoding transporters or an equivalent volume of water as a negative control. A minimum of 3 days after injection, oocytes were incubated for 10 min in uptake solutions containing ^{3}H-L-substrates (PerkinElmer) ± GPNA where specified, in ND96. Oocytes were subsequently rinsed three times in ice-cold ND96. Cells were then lysed in 1 M NaOH and 1% SDS. ^{3}H-L-substrate uptake was measured by scintillation counting using Opti-Phase HiSafe 3 (PerkinElmer) and a Trilux beta counter (PerkinElmer). Raw data from each oocyte were normalized to the mean response from the corresponding positive control (all normalized datapoints shown). Inhibition–response data generated using uptake were fit as detailed previously.

Counter-transport experiments

For counter-transport (efflux) experiments using ASCT2, methods were as follows. A minimum of 3 days after injection with RNA/water as detailed previously, oocytes were injected with a sufficient volume of ^{3}H-L-glutamine to observe >10,000 CPM by scintillation counting. After preloading with ^{3}H-L-glutamine, oocytes were immediately stored in ice-cold efflux buffer (ND96). To commence efflux, single oocytes were incubated in 400 μl room temperature efflux solutions, then rinsed three times, lysed, and counted. Efflux solutions were also counted. Percentage efflux for each oocyte was calculated using the formula,

$$\text{Efflux } (\%) = 100 \times \frac{S}{S + O},$$

where O is counts from the oocyte and S is counts from the corresponding solution. For efflux experiments using EAATs, the same methods were used, except oocytes were preloaded *via* a 30 min preincubation in [^{14}C]-labeled aspartate, rather than *via* injection.

Data availability

Raw data are available from the corresponding author upon request.

Acknowledgments—We thank Professor R. Vandenberg, Dr L. Salvati Manni, and members of the Transporter Biology Group for helpful discussions and those that support the X. laevis colony at the University of Sydney.

Author contributions—N. J. F., C. B., and R. M. R. conceptualization; N. J. F. and C. B. formal analysis; N. J. F. and C. B. investigation; N. J. F. and C. B. writing–original draft; N. J. F., C. B., and R. M. R. writing–review & editing; N. J. F. and C. B. visualization; R. M. R. supervision; R. M. R. funding acquisition.

Funding and additional information—This work was supported by the Australian National Health and Medical Research Council Project grant (grant no.: APP1164494 (to R. M. R.)), a Research Training Program Scholarships (to N. J. F.), and a Faculty of Medicine and Health Executive Dean Stipend Scholarship (to C. B.).

Conflict of interest—The authors declare that they have no conflicts of interest with the contents of this article.

Abbreviations—The abbreviations used are: ASCT, alanine serine cysteine transporter; ClCS, Cl^-conducting state; DL-TBOA, DL-threo-beta-benzyloxyaspartate; EAAT, excitatory amino acid transporter; GPNA, L-γ-glutamyl-*p*-nitroanilide; hASCT2, human ASCT2; HP2, hairpin loop 2; I, current; I_{max}, the predicted maximal current elicited by the given compound; LAT, large-neutral amino acid transporter; Na^+, sodium; ND96, 96 mM NaCl, 2 mM KCl, 1 mM $MgCl_2$, 1.8 mM $CaCl_2$, 5 mM hemisodium–Hepes, pH 7.5; rASCT2, rat ASCT2; SLC1A, solute carrier 1A; SNAT, sodium-coupled neutral amino acid transporter.

References

1. Utsunomiya-Tate, N., Endou, H., and Kanai, Y. (1996) Cloning and functional characterization of a system ASC-like Na+-dependent neutral amino acid transporter. *J. Biol. Chem.* **271**, 14883–14890
2. Arriza, J. L., Kavanaugh, M. P., Fairman, W. A., Wu, Y.-N., Murdoch, G. H., North, R. A., *et al.* (1993) Cloning and expression of a human neutral amino acid transporter with structural similarity to the glutamate transporter gene family. *J. Biol. Chem.* **268**, 15329–15332
3. Scalise, M., Console, L., Cosco, J., Pochini, L., Galluccio, M., and Indiveri, C. (2021) ASCT1 and ASCT2: brother and sister? *SLAS Discov.* **26**, 1148–1163
4. Bhutia, Y. D., and Ganapathy, V. (2016) Glutamine transporters in mammalian cells and their functions in physiology and cancer. *Biochim. Biophys. Acta* **1863**, 2531–2539
5. Freidman, N., Chen, I., Wu, Q., Briot, C., Holst, J., Font, J., *et al.* (2020) Amino acid transporters and exchangers from the SLC1A family: structure, mechanism and roles in physiology and cancer. *Neurochem. Res.* **45**, 1268–1286
6. Jiang, H., Zhang, N., Tang, T., Feng, F., Sun, H., and Qu, W. (2020) Target the human alanine/serine/cysteine transporter 2(ASCT2): achievement and future for novel cancer therapy. *Pharmacol. Res.* **158**, 104844
7. Zhang, H., Cui, K., Yao, S., Yin, Y., Liu, D., and Huang, Z. (2021) Comprehensive molecular and clinical characterization of SLC1A5 in human cancers. *Pathol. Res. Pract.* **224**, 153525
8. Jin, L., Alesi, G. N., and Kang, S. (2016) Glutaminolysis as a target for cancer therapy. *Oncogene* **35**, 3619–3625
9. Wise, D. R., DeBerardinis, R. J., Mancuso, A., Sayed, N., Zhang, X. Y., Pfeiffer, H. K., *et al.* (2008) Myc regulates a transcriptional program that stimulates mitochondrial glutaminolysis and leads to glutamine addiction. *Proc. Natl. Acad. Sci. U. S. A.* **105**, 18782–18787
10. Yuneva, M., Zamboni, N., Oefner, P., Sachidanandam, R., and Lazebnik, Y. (2007) Deficiency in glutamine but not glucose induces MYC-dependent apoptosis in human cells. *J. Cell Biol.* **178**, 93–105
11. Malik, A. R., and Willnow, T. E. (2019) Excitatory amino acid transporters in physiology and disorders of the central nervous system. *Int. J. Mol. Sci.* **20**, 5671
12. Canul-Tec, J. C., Assal, R., Cirri, E., Legrand, P., Brier, S., Chamot-Rooke, J., *et al.* (2017) Structure and allosteric inhibition of excitatory amino acid transporter 1. *Nature* **544**, 446–451
13. Garaeva, A. A., Oostergetel, G. T., Gati, C., Guskov, A., Paulino, C., and Slotboom, D. J. (2018) Cryo-EM structure of the human neutral amino acid transporter ASCT2. *Nat. Struct. Mol. Biol.* **25**, 515–521
14. Fairman, W. A., Vandenberg, R. J., Arriza, J. L., Kavanaugh, M. P., and Amara, S. G. (1995) An excitatory amino-acid transporter with properties of a ligand-gated chloride channel. *Nature* **375**, 599–603
15. Chen, I., Pant, S., Wu, Q., Cater, R. J., Sobti, M., Vandenberg, R. J., *et al.* (2021) Glutamate transporters have a chloride channel with two hydrophobic gates. *Nature* **591**, 327–331
16. Zerangue, N., and Kavanaugh, M. P. (1996) ASCT-1 is a neutral amino acid exchanger with chloride channel activity. *J. Biol. Chem.* **271**, 27991–27994
17. Broer, A., Wagner, C., Florian, L., and Broer, S. (2000) Neutral amino acid transporter ASCT2 displays substrate-induced Na+ exchange and a substrate-gated anion conductance. *Biochem. J.* **346**, 705–710
18. Wadiche, J. I., and Kavanaugh, M. P. (1998) Macroscopic and microscopic properties of a cloned glutamate transporter/chloride channel. *J. Neurosci.* **18**, 7650–7661
19. Grewer, C., and Grabsch, E. (2004) New inhibitors for the neutral amino acid transporter ASCT2 reveal its Na+-dependent anion leak. *J. Physiol.* **557**, 747–759
20. Wadiche, J. I., Amara, S. G., and Kavanaugh, M. P. (1995) Ion fluxes associated with excitatory amino acid transport. *Neuron* **15**, 721–728
21. Zerangue, N., and Kavanaugh, M. P. (1996) Flux coupling in a neuronal glutamate transporter. *Nature* **383**, 634–637
22. Scopelliti, A. J., Heinzelmann, G., Kuyucak, S., Ryan, R. M., and Vandenberg, R. J. (2014) Na+ interactions with the neutral amino acid transporter ASCT1. *J. Biol. Chem.* **289**, 17468–17479
23. Boudker, O., Ryan, R. M., Yernool, D., Shimamoto, K., and Gouaux, E. (2007) Coupling substrate and ion binding to extracellular gate of a sodium-dependent aspartate transporter. *Nature* **445**, 387–393
24. Esslinger, C. S., Cybulski, K. A., and Rhoderick, J. F. (2005) Ngamma-aryl glutamine analogues as probes of the ASCT2 neutral amino acid transporter binding site. *Bioorg. Med. Chem.* **13**, 1111–1118
25. Schulte, M. L., Dawson, E. S., Saleh, S. A., Cuthbertson, M. L., and Manning, H. C. (2015) 2-Substituted Ngamma-glutamylanilides as novel probes of ASCT2 with improved potency. *Bioorg. Med. Chem. Lett.* **25**, 113–116
26. Schulte, M. L., Fu, A., Zhao, P., Li, J., Geng, L., Smith, S. T., *et al.* (2018) Pharmacological blockade of ASCT2-dependent glutamine transport leads to antitumor efficacy in preclinical models. *Nat. Med.* **24**, 194–202
27. Bröer, A., Fairweather, S., and Bröer, S. (2018) Disruption of amino acid homeostasis by novel ASCT2 inhibitors involves multiple targets. *Front. Pharmacol.* **9**, 785
28. [preprint] Lyda, B. R., Leary, G. P., Farnsworth, J., Silvius, D., Seaver, B., Esslinger, C. S., *et al.* (2021) Discovery and synthesis of hydroxy-L-proline based blockers of the neutral amino acid transporters SLC1A4 (ASCT1) and SLC1A5 (ASCT2). *bioRxiv*. https://doi.org/10.1101/2021.12.14.470456
29. Garibsingh, R. A., Ndaru, E., Garaeva, A. A., Shi, Y., Zielewicz, L., Zakrepine, P., *et al.* (2021) Rational design of ASCT2 inhibitors using an integrated experimental-computational approach. *Proc. Natl. Acad. Sci. U. S. A.* **118**, e2104093118
30. Broer, A., Rahimi, F., and Broer, S. (2016) Deletion of amino acid transporter ASCT2 (SLC1A5) reveals an essential role for transporters SNAT1 (SLC38A1) and SNAT2 (SLC38A2) to sustain glutaminolysis in cancer cells. *J. Biol. Chem.* **291**, 13194–13205
31. Chiu, M., Sabino, C., Taurino, G., Bianchi, M. G., Andreoli, R., Giuliani, N., *et al.* (2017) GPNA inhibits the sodium-independent transport system L for neutral amino acids. *Amino Acids* **49**, 1365–1372
32. Scopelliti, A. J., Font, J., Vandenberg, R. J., Boudker, O., and Ryan, R. M. (2018) Structural characterisation reveals insights into substrate recognition by the glutamine transporter ASCT2/SLC1A5. *Nat. Commun.* **9**, 38
33. Corti, A., Dominici, S., Piaggi, S., Belcastro, E., Chiu, M., Taurino, G., *et al.* (2019) γ-Glutamyltransferase enzyme activity of cancer cells modulates L-γ-glutamyl-p-nitroanilide (GPNA) cytotoxicity. *Sci. Rep.* **9**, 891
34. Prevarskaya, N., Skryma, R., and Shuba, Y. (2018) Ion channels in cancer: are cancer hallmarks oncochannelopathies? *Physiol. Rev.* **98**, 559–621
35. Morishita, K., Watanabe, K., and Ichijo, H. (2019) Cell volume regulation in cancer cell migration driven by osmotic water flow. *Cancer Sci.* **110**, 2337–2347
36. Zander, C. B., Albers, T., and Grewer, C. (2013) Voltage-dependent processes in the electroneutral amino acid exchanger ASCT2. *J. Gen. Physiol.* **141**, 659–672

37. MacAulay, N., Gether, U., Klaerke, D. A., and Zeuthen, T. (2001) Water transport by the human Na+-coupled glutamate cotransporter expressed in Xenopus oocytes. *J. Physiol.* **530**, 367–378
38. Pant, S., Wu, Q., Ryan, R., and Tajkhorshid, E. (2022) Microscopic characterization of the chloride permeation pathway in the human excitatory amino acid transporter 1 (EAAT1). *ACS Chem. Neurosci.* **13**, 776–785
39. Vandenberg, R. J., Handford, C. A., Campbell, E. M., Ryan, R. M., and Yool, A. J. (2011) Water and urea permeation pathways of the human excitatory amino acid transporter EAAT1. *Biochem. J.* **439**, 333–340
40. Untiet, V., Kovermann, P., Gerkau, N. J., Gensch, T., Rose, C. R., and Fahlke, C. (2017) Glutamate transporter-associated anion channels adjust intracellular chloride concentrations during glial maturation. *Glia* **65**, 388–400
41. Winter, N., Kovermann, P., and Fahlke, C. (2012) A point mutation associated with episodic ataxia 6 increases glutamate transporter anion currents. *Brain* **135**, 3416–3425
42. Wu, Q., Akhter, A., Pant, S., Cho, E., Zhu, J. X., Garner, A. R., *et al.* (2022) Ataxia-linked SLC1A3 mutations alter EAAT1 chloride channel activity and glial regulation of CNS function. *J. Clin. Invest.* **132**, e154891
43. de Groot, J. F., Liu, T. J., Fuller, G., and Yung, W. K. (2005) The excitatory amino acid transporter-2 induces apoptosis and decreases glioma growth *in vitro* and *in vivo*. *Cancer Res.* **65**, 1934–1940
44. Ye, Z. C., Rothstein, J. D., and Sontheimer, H. (1999) Compromised glutamate transport in human glioma cells: reduction-mislocalization of sodium-dependent glutamate transporters and enhanced activity of cystine-glutamate exchange. *J. Neurosci.* **19**, 10767–10777
45. Varini, K., Benzaria, A., Taieb, N., Di Scala, C., Azmi, A., Graoudi, S., *et al.* (2012) Mislocalization of the exitatory amino-acid transporters (EAATs) in human astrocytoma and non-astrocytoma cancer cells: effect of the cell confluence. *J. Biomed. Sci.* **19**, 10
46. Bacci, M., Lorito, N., Ippolito, L., Ramazzotti, M., Luti, S., Romagnoli, S., *et al.* (2019) Reprogramming of amino acid transporters to support aspartate and glutamate dependency sustains endocrine resistance in breast cancer. *Cell Rep.* **28**, 104–118.e8
47. Tao, J., Deng, N. T., Ramnarayanan, K., Huang, B., Oh, H. K., Leong, S. H., *et al.* (2011) CD44-SLC1A2 gene fusions in gastric cancer. *Sci. Transl. Med.* **3**, 77ra30
48. Garcia-Bermudez, J., Baudrier, L., La, K., Zhu, X. G., Fidelin, J., Sviderskiy, V. O., *et al.* (2018) Aspartate is a limiting metabolite for cancer cell proliferation under hypoxia and in tumours. *Nat. Cell Biol.* **20**, 775–781
49. Tajan, M., Hock, A. K., Blagih, J., Robertson, N. A., Labuschagne, C. F., Kruiswijk, F., *et al.* (2018) A role for p53 in the adaptation to glutamine starvation through the expression of SLC1A3. *Cell Metab.* **28**, 721–736.e6
50. Wang, X., Chen, Z., Xu, J., Tang, S., An, N., Jiang, L., *et al.* (2022) SLC1A1-mediated cellular and mitochondrial influx of R-2-hydroxyglutarate in vascular endothelial cells promotes tumor angiogenesis in IDH1-mutant solid tumors. *Cell Res.* https://doi.org/10.1038/s41422-022-00650-w
51. Reyes, N., Ginter, C., and Boudker, O. (2009) Transport mechanism of a bacterial homologue of glutamate transporters. *Nature* **462**, 880–885
52. Garaeva, A. A., Guskov, A., Slotboom, D. J., and Paulino, C. (2019) A one-gate elevator mechanism for the human neutral amino acid transporter ASCT2. *Nat. Commun.* **10**, 3427
53. Colas, C., Grewer, C., Otte, N. J., Gameiro, A., Albers, T., Singh, K., *et al.* (2015) Ligand discovery for the alanine-serine-cysteine transporter (ASCT2, SLC1A5) from homology modeling and virtual screening. *PLoS Comput. Biol.* **11**, e1004477
54. Seal, R. P., Shigeri, Y., Eliasof, S., Leighton, B. H., and Amara, S. G. (2001) Sulfhydryl modification of V449C in the glutamate transporter EAAT1 abolishes substrate transport but not the substrate-gated anion conductance. *Proc. Natl. Acad. Sci. U. S. A.* **98**, 15324–15329
55. Ryan, R. M., and Vandenberg, R. J. (2002) Distinct conformational states mediate the transport and anion channel properties of the glutamate transporter EAAT-1. *J. Biol. Chem.* **277**, 13494–13500
56. Shabaneh, M., Rosental, N., and Kanner, B. I. (2014) Disulfide cross-linking of transport and trimerization domains of a neuronal glutamate transporter restricts the role of the substrate to the gating of the anion conductance. *J. Biol. Chem.* **289**, 11175–11182
57. Jiang, J., Shrivastava, I. H., Watts, S. D., Bahar, I., and Amara, S. G. (2011) Large collective motions regulate the functional properties of glutamate transporter trimers. *Proc. Natl. Acad. Sci. U. S. A.* **108**, 15141–15146
58. Scalise, M., Pochini, L., Panni, S., Pingitore, P., Hedfalk, K., and Indiveri, C. (2014) Transport mechanism and regulatory properties of the human amino acid transporter ASCT2 (SLC1A5). *Amino Acids* **46**, 2463–2475
59. Jumper, J., Evans, R., Pritzel, A., Green, T., Figurnov, M., Ronneberger, O., *et al.* (2021) Highly accurate protein structure prediction with AlphaFold. *Nature* **596**, 583–589
60. Del Alamo, D., Sala, D., McHaourab, H. S., and Meiler, J. (2022) Sampling alternative conformational states of transporters and receptors with AlphaFold2. *Elife* **11**, e75751
61. Poulsen, M. V., and Vandenberg, R. J. (2001) Niflumic acid modulates uncoupled substrate-gated conductances in the human glutamate transporter EAAT4. *J. Physiol.* **534**, 159–167
62. Schrödinger, LLC (2019) *The PyMOL Molecular Graphics System, Version 2.0*, Schrödinger, LLC, New York, NY